

Acceleration techniques for optimization over trained neural network ensembles

Keliang Wang

Department of Operations and Information Management, School of Business, University of Connecticut

Leonardo Lozano

Operations, Business Analytics & Information Systems, University of Cincinnati

Carlos Cardonha

Department of Operations and Information Management, School of Business, University of Connecticut

David Bergman

Department of Operations and Information Management, School of Business, University of Connecticut

Abstract

We study optimization problems where the objective function is modeled through feedforward neural networks with rectified linear unit (ReLU) activation. Recent literature has explored the use of a single neural network to model either uncertain or complex elements within an objective function. However, it is well known that ensembles of neural networks produce more stable predictions and have better generalizability than models with single neural networks, which suggests the application of ensembles of neural networks in a decision-making pipeline. We study how to incorporate a neural network ensemble as the objective function of an optimization model and explore computational approaches for the ensuing problem. We present a mixed-integer linear program based on existing popular big- M formulations for optimizing over a single neural network. We develop two acceleration techniques for our model, the first one is a preprocessing procedure to tighten bounds for critical neurons in the neural network while the second one is a set of valid inequalities based on Benders decomposition. Experimental evaluations of our solution methods are conducted on one global optimization problem and two real-world data sets; the results suggest that our optimization algorithm outperforms the adaption of an state-of-the-art approach in terms of computational time and optimality gaps.

1 Introduction

Finding effective ways of embedding neural networks (NNs) within optimization problems can provide significant improvements in automated decision making. The potential for application of such a framework already exists in the literature and in practice, and arises in three contexts:

1. Unknown objective. E.g., suppose the revenue for a product is a function of advertising budget and cost, and is modeled through a NN trained from historical data. Identifying the optimal budget and cost requires embedding the NN in the optimization model.
2. Non-linearity. If a function does not admit an exact linear representation, a surrogate model for a global optimization problem can be trained from simulated inputs. This surrogate model, in the form of a NN, can then be used as the objective function.
3. Obfuscation. For example, a firm wants to keep information hidden so instead of producing an interpretable model it trains a NN, which then must be used within an optimization problem, either as a part of the objective or the constraints.

Based on the generality of application, finding effective ways of handling NNs within an optimization problem opens the door for enhanced decision making capability. A major issue is immediately realized: can we trust the output from the NN model at the solution identified by an optimizer? NNs have a tendency to produce highly variable predictions, even for minor changes in inputs, and so optimization problems where the features are variables poses significant risks.

To address the challenge of highly variable outputs from NNs, we explore in this paper the use of ensemble of NNs in optimization problems instead of single NNs (a preliminary version of this work appears in a recent conference paper that we published (Wang et al. 2021)). It is well known that ensembles can produce competitive predictive accuracy compared to a single NN but with lower variability and better generalization ability (Dietterich 2000, Zhou et al. 2002), therefore suggesting that their use is particularly well suited for a decision making pipeline. However, this leads to a challenging optimization problem; optimizing over one NN can be time consuming (Anderson et al. 2020), and existing models lead to even more computational bottlenecks in the case of ensemble.

As a motivating example we consider **Peaks**, a commonly used test problem for global non-linear optimization (defined in (15)), which has a known global minimum objective function value of -6.551 . We train a single neural network and an ensemble of neural networks to learn the highly nonlinear objective function using standard parameter selection techniques based on simulated input data (more experiments related to simulating data to build surrogate models will be given in an experimental results section later in the paper). We then optimize over the trained predictor and replicate the procedure 10 times to obtain confidence intervals (CI) and mean values for the optimal value returned by the optimization models. The 95% CI for the model based on a single NN is $[-6.527, -6.467]$, with mean equal to -6.497 . For the model based on an ensemble we obtain a 95% CI of $[-6.541, -6.498]$, with mean of -6.520 , which is narrower and closer to the actual global minimum. This example highlights that the superior stability and predictive capabilities of NN ensembles likely translates into better optimization results.

Our focus in this study is therefore to:

- Introduce the use of ensemble to replace single NN modeling within a optimization decision pipeline, thereby alleviating the issue of variability in predictions; and
- Investigate algorithmic enhancements for optimization models with embedded NNs ensembles.

More formally and specifically, the problem we study is as follows. Given a function f , let $\mathcal{E}_f = \{N^1, N^2, \dots, N^e\}$ be an ensemble of e NNs representing f and Ω be the feasible set of possible inputs to the ensemble. In general, an ensemble is built in two steps: a method to train multiple estimators and the approach to combine their predictions. We adopt the popular Bagging method (Breiman 1996) for training NNs and use the averaging method to combine predictions. An estimate of f for any point x in Ω produced by \mathcal{E}_f is given by the average of the individual estimates of each neural network in \mathcal{E}_f , that is,

$$\mathcal{E}_f(x) = \frac{1}{e} \sum_{i=1}^e N^i(x).$$

We study the following problem:

$$\max_{x \in \Omega} \mathcal{E}_f(x) \tag{1}$$

In this work, we adapt an existing big- M integer programming formulation (Fischetti and Jo 2018, Cheng et al. 2017, Anderson et al. 2020) and propose two acceleration strategies to solve Problem 1. The first one is a preprocessing procedure that seeks to strengthen the baseline formulation by finding strong bounds for variables associated with a subset of critical nodes. The second strategy is a set of valid inequalities derived from Benders optimality cuts for a decomposition of the problem. We assess the performance of our algorithms using three benchmark instances: the *peaks* function, which has been traditionally used by the global optimization community, the *wine* data set introduced by Cortez et al. (2009), and the *concrete* data set, which

was introduced by Yeh (1998) and has also been used in the optimization literature (Mišić 2020). The results exhibit a superiority of our algorithm over a benchmark state-of-the-art branch-and-cut approach in terms of computational performance.

The remainder of the paper is organized as follows. After providing a literature review in Section 2, we introduce the notation and a baseline model in Section 3. Section 4 presents our proposed acceleration techniques. We present the results of our experiments in Section 5 and conclude with directions for future work in Section 6.

2 Literature Review

We investigate a category of problems that integrates predictive models and optimization. In this framework, components of the objective function are represented (or approximated) by a Machine Learning model $\hat{f}(x, \theta)$, characterized by a vector θ of fixed parameters and a vector x of input features, whose values can be selected and optimized by the underlying optimization model.

Previous works from the literature use a similar algorithmic framework. Bertsimas et al. (2016) optimize over a ridge regression to recommend effective treatments for cancer. Liu et al. (2020) use linear estimators of travel times in order to optimize real-time order assignments for a food service provider. Other examples can be found in scholarship allocation for admitted students to maximize class size (Bergman et al. 2019), personalized pricing to maximize revenue (Biggs et al. 2021), and ordering of the items to sell in an auction to maximize expected revenue (Verwer et al. 2017).

As embedding predictive models into optimization formulations is a critical aspect of this framework, previous literature has focused on predictive models that can be linearized and formulated as a mixed-integer linear programs (MILP), such as logistic regression, linear models, decision trees, random forests, and neural networks with Rectified Linear Unit (ReLU) activation functions (Bergman et al. 2019, Verwer et al. 2017, Biggs et al. 2017, Mišić 2020). Some predictive models and their regularized versions lead to easier optimization problems and are chosen to eschew computational intractability (Liu et al. 2020, Bertsimas et al. 2016, Xiao et al. 2019). On the other hand, some predictive models result in challenging optimization problems. For example, it has been proved that the problem of maximizing (or minimizing) the output of random forests or neural networks is NP-hard (Mišić 2020, Katz et al. 2017). In particular, Mišić (2020) develops two solution methods, based on Benders decomposition, that exploit the special structure of decision trees to speedup the solution of optimization models related to large-sized random forests.

Recent studies on solving optimization models with embedded neural networks have explored different techniques to encode neural networks. Schweidtmann and Mitsos (2019) study neural networks with hyperbolic tangent (\tanh) activation functions to solve deterministic global optimization problems; the formulation is solved by a customized branch-and-bound based solver that relies on McCormick relaxations of the \tanh activation functions. Bartolini et al. (2011) propose so-called *Neuron Constraints* to incorporate NN formulations into a constraint programming approach (Bartolini et al. 2011). Recent work has focused mainly on neural networks with ReLU activation functions, in part because (1) the ReLU function is recommended as a default activation when training neural networks, as it performs well in widespread applications (Goodfellow et al. 2016); and (2) the piecewise linear nature of ReLU admits a relatively simple big- M formulation that is easily incorporated within MILP models.

Among a number of works that integrate MILP with ReLU neural networks, one line of research from the machine learning community is under rapid development and concentrates on using MILP to verify certain properties of neural networks. These verification problems appear in different formats, e.g. reachability analysis of NNs (Lomuscio and Maganti 2017), robustness of NNs to adversarial inputs (Cheng et al. 2017, Tjeng et al. 2019, Xiao et al. 2019, Fischetti and Jo 2018), and output range of a trained NN (Dutta et al. 2018). Although the works mentioned above present different problems, their formulations are expressed essentially as an MILP (see

also Bunel et al. (2018), Botoeva et al. (2020)). Besides NNs verification, MILP is also used for reducing the size of trained neural networks (lossless compression) in Serra et al. (2020) and finding the expressiveness of NNs (Serra et al. 2018).

Furthermore, different techniques have been explored to speed up the solution times for NN-embedded optimization models. As the constant values used in big- M formulations affect the strength of a problem formulation and, consequently, its solution time (Vielma 2015), several papers conduct pre-processing procedures to identify tighter bounds for the big- M values (Cheng et al. 2017, Dutta et al. 2018, Tjeng et al. 2019, Fischetti and Jo 2018, Grimstad and Andersson 2019). We discuss this methods in detail in Section 4 as they are closely related to our proposed techniques. Bunel et al. (2018) split the input domain to form smaller MILPs restricted to each part of the solution space. Botoeva et al. (2020) define dependency relations between neurons in terms of their activation (or deactivation) and explore them to derive cuts that reduce the search space. Anderson et al. (2020) propose an exponentially-sized convex hull formulation for a single neuron and provide an efficient separation procedure to find the most violated inequality at any given fractional point. Tsay et al. (2021) extend the work of Anderson et al. (2020) by partitioning the input vector of a ReLU function into groups and considering convex hull formulations over the partitions via disjunctive programming. Depending on the number of partitions, their formulation is able to approximate the convex hull of a ReLU function with fewer number of constraints and auxiliary variables than the ideal formulation of Anderson et al. (2020).

Finally, successful applications of ensemble learning can be found in numerous data science competitions nowadays. Dietterich (2000) provides statistical, computational and representational arguments to show that an ensemble is always able to outperform each of its individual component estimators. Ensembles of neural network were introduced by Hansen and Salamon (1990) and have gained substantial development over the last years (See Li et al. (2018) for a detailed survey).

3 Basic Optimization Model

We now present our baseline optimization model, which was first proposed in Wang et al. (2021) and is a straightforward extension of existing MIP models for optimizing over a single NN (see e.g., Fischetti and Jo (2018)). Consider an ensemble $\mathcal{N} \equiv \{N_1, \dots, N_e\}$ of e neural networks. Each NN is a layered graph and we refer to each vertex in a NN as a neuron. Let L_i denote the number of layers and n_l^i denote the number of neurons in the l -th layer of N_i , $i \in \{1, \dots, e\}$. We use vector $(n_1^i, \dots, n_{L_i}^i)$ to succinctly represent the architecture of N_i and assume that $n_{L_i}^i = 1$ for all $i \in \{1, \dots, e\}$, i.e., there is only one neuron in the output layer of each NN in \mathcal{N} . We refer to $\{2, 3, \dots, L_i - 1\}$ as the set of intermediate layers of N_i , i.e., all layers except the first and the last. Finally, the neural networks of \mathcal{N} do not share neurons or arcs, so the description of each NN N_i of \mathcal{N} , described next, provides a complete characterization of the ensemble.

Let $v_j^{i,l}$ denote the j^{th} neuron in layer l of N_i . Each $v_j^{i,l}$ receives a series of inputs and produces a single (scalar) output $y_j^{i,l}$. For the j -th neuron of the first layer, both its input and its output is the j -th coordinate of x , i.e., $v_j^{i,1}$ receives x_j , the j^{th} component of the decision variables vector, and returns

$$y_j^{i,1} = x_j.$$

Observe that all NNs of an ensemble \mathcal{N} must have the same number of nodes in the first layer, so we occasionally simplify the notation by dropping the reference to the NN and use n_1 instead of n_1^i .

Each neuron $v_j^{i,l}$ of an intermediate layer l receives a vector of inputs $\mathbf{y}^{i,l-1} \equiv [y_1^{i,l-1}, \dots, y_{n_{l-1}^i}^{i,l-1}]$, given by the outputs of the neurons in the previous layer. The output $y_j^{i,l}$ of $v_j^{i,l}$ is defined as

$$y_j^{i,l} = \text{ReLU} \left((\mathbf{W}_j^{i,l})^\top \mathbf{y}^{i,l-1} + b_j^{i,l} \right), \quad (2)$$

where $\text{ReLU} : \mathbb{R} \rightarrow \mathbb{R}^+$ is the Rectified Linear Unit (ReLU) activation function, defined as $\text{ReLU}(\bullet) \equiv \max(0, \bullet)$. $\mathbf{W}_j^{i,l} \in \mathbb{R}^{n_{i-1}}$ is a *weight* vector and $b_j^{i,l} \in \mathbb{R}$ is a *bias* scalar. Both $\mathbf{W}_j^{i,l}$ and $b_j^{i,l}$ are generated during the training process of N_i and, for the purpose of optimization over \mathcal{N} , they are fixed (i.e., these values cannot be modified).

Finally, the output y_1^{i,L_i} of v_1^{i,L_i} , the single terminal neuron in the last layer of N_i , is computed as an affine combination of the previous layer's output without applying the ReLU function, i.e.,

$$y_1^{i,L_i} = (\mathbf{W}_1^{i,L_i})^\top \mathbf{y}^{i,L_i-1} + b_1^{i,L_i}.$$

3.1 Formulation of ReLU functions

The fundamental building block of our formulation is a mathematical programming representation of the ReLU function for a single neuron, which has been widely used in the literature (Fischetti and Jo 2018, Tjeng et al. 2019, Anderson et al. 2020). For each neuron $v_j^{i,l}$, we define an auxiliary continuous variable $h_j^{i,l}$ to capture the linear component of Expression 2, which is the value of the affine combination of the neuron's inputs before applying the ReLU function (also known as the *preactivation*). Additionally, we define a binary variable $z_j^{i,l}$ that takes a value of 1 if $v_j^{i,l}$ is *active* (i.e., its output is strictly greater than 0). Finally, assume that a lower bound $\text{LB}_j^{i,l} < 0$ and upper bound $\text{UB}_j^{i,l} > 0$ are known for each $h_j^{i,l}$, i.e., $h_j^{i,l} \in [\text{LB}_j^{i,l}, \text{UB}_j^{i,l}]$; observe that neurons for which both bounds are either non-positive or non-negative can be removed or merged (Serra et al. 2020). A MILP formulation that models the behaviour of $v_j^{i,l}$ is given by:

$$h_j^{i,l} = (\mathbf{W}_j^{i,l})^\top \mathbf{y}^{i,l-1} + b_j^{i,l} \quad (3a)$$

$$h_j^{i,l} \leq y_j^{i,l} \leq h_j^{i,l} + |\text{LB}_j^{i,l}|(1 - z_j^{i,l}) \quad (3b)$$

$$0 \leq y_j^{i,l} \leq \text{UB}_j^{i,l} z_j^{i,l} \quad (3c)$$

$$z_j^{i,l} \in \{0, 1\} \quad (3d)$$

$$h_j^{i,l}, y_j^{i,l} \in \mathbb{R} \quad (3e)$$

Constraint (3a) sets the value of $h_j^{i,l}$. Constraints (3b)–(3c) ensure that if $h_j^{i,l} > 0$, then $y_j^{i,l} = h_j^{i,l}$ and $z_j^{i,l} = 1$, i.e., they enforce that the output equals the evaluation of the ReLU function.

Observe that $\text{LB}_j^{i,l}$ and $\text{UB}_j^{i,l}$ act as big- M constants in (3b) and (3c), respectively. Therefore, the strength of Formulation (3) for $v_j^{i,l}$ strongly depends on the values of $\text{LB}_j^{i,l}$ and $\text{UB}_j^{i,l}$. One of the main contributions of this work is a strategy to compute tighter bounds, which we present in §4.1.

3.2 MILP formulation for optimization over ensemble

We now present an MILP formulation for optimizing over a given ensemble \mathcal{N} , which is a straightforward adaptation of Model (3) over the complete set of neurons in \mathcal{N} .

$$\max \quad \frac{1}{e} \sum_{i=1}^e y_1^{i,L_i} \quad (4a)$$

$$\text{s.t.} \quad y_j^{i,1} = x_j \quad \forall i \in \{1, \dots, e\}, j \in \{1, \dots, n_1\} \quad (4b)$$

$$y_1^{i,L_i} = h_1^{i,L_i} \quad \forall i \in \{1, \dots, e\} \quad (4c)$$

$$h_j^{i,l} = (\mathbf{W}_j^{i,l})^\top \mathbf{y}^{i,l-1} + b_j^{i,l} \quad \forall i \in \{1, \dots, e\}, l \in \{2, \dots, L_i\}, j \in \{1, \dots, n_l\} \quad (4d)$$

$$h_j^{i,l} \leq y_j^{i,l} \leq h_j^{i,l} + |\text{LB}_j^{i,l}|(1 - z_j^{i,l}) \quad \forall i \in \{1, \dots, e\}, l \in \{2, \dots, L_i - 1\}, j \in \{1, \dots, n_l^i\} \quad (4e)$$

$$0 \leq y_j^{i,l} \leq \text{UB}_j^{i,l} z_j^{i,l} \quad \forall i \in \{1, \dots, e\}, l \in \{2, \dots, L_i - 1\}, j \in \{1, \dots, n_l^i\} \quad (4f)$$

$$z_j^{i,l} \in \{0, 1\} \quad \forall i \in \{1, \dots, e\}, l \in \{2, \dots, L_i - 1\}, j \in \{1, \dots, n_l^i\} \quad (4g)$$

$$h_j^{i,l}, y_j^{i,l} \in \mathbb{R} \quad \forall i \in \{1, \dots, e\}, l \in \{1, \dots, L_i\}, j \in \{1, \dots, n_l^i\} \quad (4h)$$

$$x \in \Omega \quad (4i)$$

Variable x corresponds to the input vector, which belongs to the (potentially constrained) set $\Omega \subseteq \mathbb{R}^{n_1}$. The objective function optimizes the average output of the last neuron in each NN. Constraints (4b) ensure that the outputs for neurons in the first layer of any NN correspond to x . Constraints (4c) set the output of the single neuron in the last layer of each NN to the affine combination of the neuron's inputs, without applying the ReLU function. Constraints (4d)–(4h) replicate Formulation (3) for each intermediate neuron in the ensemble.

3.3 Baseline algorithm

Anderson et al. (2020) investigate Formulation (3) and provide a convex hull formulation (also referred to as a sharp formulation) in the space of the original variables with an exponential number of constraints. They propose a branch-and-cut algorithm (B&C) which iteratively finds and adds the most violated constraints at fractional solutions obtained during the exploration of the branch-and-bound tree. To the best of our knowledge, B&C is the state-of-the-art approach for optimizing over a single neural network.

As Formulation (4) is also based on Formulation (3), B&C can be directly adapted to solve our problem. As a result, we use B&C as a baseline benchmark algorithm to compare against and measure the effects of our proposed acceleration techniques in §5.

4 Model Enhancements

We propose two acceleration strategies to enhance Formulation (4). The first strategy focuses on obtaining strong values for $\text{LB}_j^{i,l}$ and $\text{UB}_j^{i,l}$ at critical neurons in the ensemble, and the second explores the incorporation of valid inequalities derived from Benders' optimality cuts. We denote by E-NN the algorithm that combines Formulation (4) with the enhancements presented in this section.

4.1 Targeted Strong Bounds

Depending on the tightness of the bounds, the output for intermediate neurons computed at fractional solutions can greatly deviate from the correct evaluation of the ReLU function in Formulation (3). We motivate the need for strong values of $\text{LB}_j^{i,l}$ and $\text{UB}_j^{i,l}$ with an example.

Example 1. Let $v_j^{i,l}$ be a neuron of an intermediate layer with $h_j^{i,l} \in [-20, 10]$. Consider the vector $(\bar{h}_j^{i,l}, \bar{y}_j^{i,l}, \bar{z}_j^{i,l})$ of values associated with $v_j^{i,l}$ composing a fractional solution to Model (3). Because the bounds are loose, the vector $(\bar{h}_j^{i,l}, \bar{y}_j^{i,l}, \bar{z}_j^{i,l}) = (-5, 5, 0.5)$ satisfies constraints (3b) and (3c), as

$$-5 \leq 5 \leq -5 + |-20|(1 - 0.5) \quad \text{and} \quad 0 \leq 5 \leq 10(0.5),$$

respectively. Observe that the correct evaluation of the ReLU function applied to $\bar{h}_j^{i,l} = -5$ is 0 (instead of 5). Conversely, if the bounds of $h_j^{i,l}$ were tightened to $[-5, 10]$, then the same

assignment $\bar{h}_j^{i,l} = -5$ could only compose a feasible solution with $\bar{y}_j^{i,l} = \bar{z}_j^{i,l} = 0$, thus yielding the correct value of $\text{ReLU}(\bar{h}_j^{i,l})$. ■

A basic procedure for computing bounds from the literature is via interval arithmetic (Cheng et al. 2017, Tjeng et al. 2019, Anderson et al. 2020). In this technique, bounds are lexicographically computed layer by layer as:

$$\text{LB}_j^{i,l} = \sum_{k \in \{1, \dots, n_{l-1}^i\}} \left(\text{LB}_k^{i,l-1} \max\{0, w_{j,k}^{i,l}\} + \text{UB}_k^{i,l-1} \min\{0, w_{j,k}^{i,l}\} \right) + b_j^{i,l}; \text{ and} \quad (5)$$

$$\text{UB}_j^{i,l} = \sum_{k \in \{1, \dots, n_{l-1}^i\}} \left(\text{UB}_k^{i,l-1} \max\{0, w_{j,k}^{i,l}\} + \text{LB}_k^{i,l-1} \min\{0, w_{j,k}^{i,l}\} \right) + b_j^{i,l}, \quad (6)$$

where $w_{j,k}^{i,l}$ denotes the scalar value at the k^{th} position of weight vector $\mathbf{W}_j^{i,l}$ and the bounds for neurons in the first layer are equal to the respective bounds for x .

Interval arithmetic is likely to result in weak bounds, as over-estimated bounds from one layer are used in the computation of the bounds for the next layer, thus propagating increasingly worse bounds through the network (Tjeng et al. 2019, Tsay et al. 2021). As an alternative to interval arithmetic, Tjeng et al. (2019) propose a so-called *progressive bounds tightening* procedure that solves up to 2 linear programs for each neuron $v_j^{i,l}$. These LPs are obtained by relaxing the integrality constraints on the z -variables and considering the objectives of maximizing and minimizing $h_j^{i,l}$. To obtain even tighter bounds, Fischetti and Jo (2018) solve 2 MILPs per neuron, obtained by considering the objectives of maximizing and minimizing $h_j^{i,l}$ for each critical neuron without relaxing the integrality constraints on the z -variables.

The bounding procedures described above offer a trade-off between the computational time required to compute the bounds and the quality of the bounds obtained. Interval arithmetic is quite efficient but provides weak bounds. On the other hand, solving 2 MILPs per neuron provide strong bounds at the expense of considerably higher computation times.

In order to offset the high computational times required to obtain strong bounds, we propose solving 2 MIPs only for *critical* neurons, which are neurons that are likely to correspond to fractional solutions for which the ReLU function evaluation is vastly overestimated. For the non-critical neurons we compute bounds by solving the 2 LPs as done by Tjeng et al. (2019) and Tsay et al. (2021). The cornerstone of our proposed bounding approach is a procedure to identify such critical neurons efficiently, which we describe next.

We start with a version of Formulation (4) that uses bounds obtained via LPs for all neurons in the neural network. After solving K nodes of the branch-and-bound tree, we stop the execution and identify critical neurons by *surveying* these nodes. Namely, for each fractional solution explored, denoted by $(\bar{x}, \bar{h}, \bar{y}, \bar{z})$, we record the *discrepancy* of each neuron at a given fractional solution as

$$\delta_j^{i,l}(\bar{h}, \bar{y}) = \begin{cases} \bar{y}_j^{i,l} & \text{if } \bar{h}_j^{i,l} < 0; \\ \bar{y}_j^{i,l} - \bar{h}_j^{i,l} & \text{if } \bar{h}_j^{i,l} \geq 0, \end{cases} \quad (7)$$

which captures the magnitude of the overestimation of the ReLU function by $(\bar{x}, \bar{h}, \bar{y}, \bar{z})$; observe that the correct evaluation of the ReLU function is 0 in the first case and $\bar{h}_j^{i,l}$ in the second case. We define critical neurons as the ones for which the total discrepancy, given by the sum of all discrepancies computed for each of the K surveyed nodes, is greater than or equal to a given threshold τ .

After identifying the critical nodes, we identify the bounds for each critical neuron by solving the 2 MILPs described above, which incorporate the integrality constraints on the z -variables and minimize and maximize $h_j^{i,l}$, respectively. Observe that, in order to compute the bounds for a neuron $v_j^{i,l}$, we only need to incorporate the nodes of the first $l-1$ layers (plus $v_j^{i,l}$) in the associated MILP, so the problem is not as large and hard as the original problem. Nevertheless, solving these sub-problems can be time-consuming, so we impose a time limit on the solution

of the bounding MILPs. When an MILP is not solved to optimality because of the time limit, we recover the best bound obtained during the optimization and use this value as an over-approximated (yet valid) substitute for the optimal objective value (as done by Fischetti and Jo (2018)). In our computational experiments we find that even for very small time limits (10 seconds or less) the best bounds from the interrupted MILPs are considerably tighter than the solutions from the LPs.

Algorithm 1 summarizes our proposed targeted strong bounds procedure.

Algorithm 1 Targeted Strong Bounds Procedure

- 1: Solve 2 LPs for each neuron to initialize the lower and upper bounds for each neuron.
 - 2: Generate Formulation (4) using the LP bounds and execute the branch-and-bound algorithm until K nodes are solved.
 - 3: Survey the K nodes and compute the discrepancies $\delta_j^{i,l}(\bar{h}, \bar{y})$ for each neuron $v_j^{i,l}$ at every fractional solution identified when solving Formulation (4) with the LP bounds.
 - 4: Identify the set of critical neurons.
 - 5: Solve 2 MILPs for the critical neurons and use best bounds identified within the time limit.
-

After computing the strengthened bounds via Algorithm 1 we solve Formulation (4) using the updated bounds. We remark that in the process of obtaining stronger bounds, it often happens that several neurons can be removed from the ensemble as it is established that they are always active (when both bounds are non-negative) or they are always inactive (when both bounds are non-positive) (Cheng et al. 2017, Serra et al. 2020).

4.2 Valid Inequalities

We propose a set of valid inequalities for Formulation (4) that can be interpreted as optimality Bender’s cuts from a Benders’ decomposition (Benders 1962). Let \mathcal{Z} be the discrete space defined by the integrality constraints (4g), and let $\mathcal{X}(z)$ be the space defined by the remaining constraints (4b)–(4f) and (4h)–(4i) for a fixed binary vector z . We reformulate Formulation (4) as

$$v^* = \max_{z \in \mathcal{Z}} \max_{(x, h, y) \in \mathcal{X}(z)} \frac{1}{e} \sum_{i=1}^e y_1^{i, L_i}, \quad (8)$$

where the outer (maximization) problem contains all the binary variables and the inner (minimization) problem is a LP parameterized by the discrete decisions of the outer problem. Because of strong duality, we can alternatively model (8) by replacing the inner maximization problem with its dual minimization problem. Let $\pi_j^{i,l}$, $\alpha_j^{i,l}$, and $\beta_j^{i,l}$ denote the dual variables associated with constraints (4d), (4e), and (4f), respectively. Let Ψ be the dual feasible space (projecting out dual variables with an objective coefficient equal to 0) and note that the dual feasible space is not parameterized by z , i.e., the set of feasible dual points remains the same independently of the discrete decisions from the outer problem. By replacing the inner problem by its dual, we can rewrite (8) as

$$v^* = \max_{z \in \mathcal{Z}} \min_{(\pi, \alpha, \beta) \in \Psi} \sum_{i=1}^e \sum_{l=2}^{L_i} \sum_{j=1}^{n_l^i} b_j^{i,l} \pi_j^{i,l} + \sum_{i=1}^e \sum_{l=2}^{L_i-1} \sum_{j=1}^{n_l^i} |\text{LB}_j^{i,l}| (1 - z_j^{i,l}) \alpha_j^{i,l} + \sum_{i=1}^e \sum_{l=2}^{L_i-1} \sum_{j=1}^{n_l^i} \text{UB}_j^{i,l} z_j^{i,l} \beta_j^{i,l}, \quad (9)$$

where the dual objective function is parameterized by the discrete decision variables z . In Proposition 1 we present our proposed valid inequalities for Formulation (4).

Proposition 1. For any feasible dual solution $(\bar{\pi}, \bar{\alpha}, \bar{\beta}) \in \Psi$, the following inequality is valid to Formulation (4):

$$\frac{1}{e} \sum_{i=1}^e y_1^{i,L_i} \leq \sum_{i=1}^e \sum_{l=2}^{L_i} \sum_{j=1}^{n_l^i} b_j^{i,l} \bar{\pi}_j^{i,l} + \sum_{i=1}^e \sum_{l=2}^{L_i-1} \sum_{j=1}^{n_l^i} |LB_j^{i,l}| (1 - z_j^{i,l}) \bar{\alpha}_j^{i,l} + \sum_{i=1}^e \sum_{l=2}^{L_i-1} \sum_{j=1}^{n_l^i} UB_j^{i,l} z_j^{i,l} \bar{\beta}_j^{i,l} \quad (10)$$

Proof. For any $\bar{z} \in \mathcal{Z}$ for which $\mathcal{X}(\bar{z}) \neq \emptyset$ define

$$v(\bar{z}) = \max_{(x,h,y) \in \mathcal{X}(\bar{z})} \frac{1}{e} \sum_{i=1}^e y_1^{i,L_i}, \quad (11)$$

and note that for any feasible primal solution $(\bar{x}, \bar{h}, \bar{y}) \in \mathcal{X}(\bar{z})$ it holds that

$$\frac{1}{e} \sum_{i=1}^e \bar{y}_1^{i,L_i} \leq v(\bar{z}). \quad (12)$$

Because of strong duality, there exists a dual solution $(\pi^*, \alpha^*, \beta^*) \in \Psi$ for which

$$v(\bar{z}) = \sum_{i=1}^e \sum_{l=2}^{L_i} \sum_{j=1}^{n_l^i} b_j^{i,l} \pi_j^{*,i,l} + \sum_{i=1}^e \sum_{l=2}^{L_i-1} \sum_{j=1}^{n_l^i} |LB_j^{i,l}| (1 - \bar{z}_j^{i,l}) \alpha_j^{*,i,l} + \sum_{i=1}^e \sum_{l=2}^{L_i-1} \sum_{j=1}^{n_l^i} UB_j^{i,l} \bar{z}_j^{i,l} \beta_j^{*,i,l}. \quad (13)$$

Because of weak duality we obtain that

$$v(\bar{z}) \leq \sum_{i=1}^e \sum_{l=2}^{L_i} \sum_{j=1}^{n_l^i} b_j^{i,l} \bar{\pi}_j^{i,l} + \sum_{i=1}^e \sum_{l=2}^{L_i-1} \sum_{j=1}^{n_l^i} |LB_j^{i,l}| (1 - \bar{z}_j^{i,l}) \bar{\alpha}_j^{i,l} + \sum_{i=1}^e \sum_{l=2}^{L_i-1} \sum_{j=1}^{n_l^i} UB_j^{i,l} \bar{z}_j^{i,l} \bar{\beta}_j^{i,l}, \quad (14)$$

for any $(\bar{\pi}, \bar{\alpha}, \bar{\beta}) \in \Psi$. This concludes the proof. ■

There exists an exponential number of valid inequalities (10). Therefore, we propose an iterative approach, where these inequalities are identified and added every time that a feasible integer solution is explored. It is also important to remark that the strength of the valid inequalities is again dependent on the quality of the lower and upper bounds.

5 Computational Results

We present in this section the results of our computational experiments. We use Python 3.7, scikit-learn 0.23.2 (Pedregosa et al. (2011)), and a 2.6 GHz 6-Core Intel i7-9750H CPU with 32 GB of RAM to create and train the neural networks composing the instances of our data sets, described in §5.1. We use Java implementations of B&C and E-NN, and we use Gurobi 9.0.2 to solve the mixed-integer programming formulations (Gurobi Optimization 2018). The experiments are executed on an Intel Xeon E5-1650 CPU (six cores) running at 3.60 GHz with 32 GB of RAM on Windows 10. Each execution is restricted by a time limit of 3,600 seconds. All code and instances are readily available upon request.

5.1 Instances

Each instance is characterized by a benchmark problem and the architecture (L, n, e) of the ensemble used to solve the problem. Tuple (L, n, e) indicates that all the e NNs in our ensemble have L intermediate layers (e.g., each NN has $L + 2$ layers in total) and n nodes per internal layer.

5.1.1 Benchmark Problems

Three different problems are used in the generation of our data sets. We describe the underlying application, the number of features, and the number of samples used to train the ensembles for each problem below.

Peaks: The peaks function $f(x, y)$ is a benchmark instance in the global optimization literature (see [Schweidtmann and Mitsos \(2019\)](#)). Peaks is defined over $[-3, 3]^2$ as

$$f(x, y) \equiv 3(1 - x^2)^2 e^{-x^2 - (y+1)^2} - 10 \left(\frac{x}{5} - x^3 - y^5 \right) e^{-x^2 - y^2} - \frac{e^{-(x+1)^2 - y^2}}{3}. \quad (15)$$

The goal is to identify a solution (x^*, y^*) such that $f(x^*, y^*)$ is minimum. The global optimal solution value is $f^* = -6.551$, which is attained at $x^* = 0.228$ and $y^* = -1.626$. In order to train a neural network that estimates f , we generate a data set by sampling 1,000 random points from $[-3, 3]^2$ and computing the exact value $f(x, y)$ for each of these points.

Wine: This first real-world application is based on the wine preference data set introduced by [Cortez et al. \(2009\)](#) (see also [Mišić \(2020\)](#)). In this work, the authors propose regression techniques to estimate the quality of a wine based on 11 attributes, such as the concentration of residual sugar and the relative volume of alcohol, using a data set with 1,599 samples. In the optimization version of the problem, we wish to identify the physicochemical properties of a wine that would have the highest quality.

Concrete: This second real-world application was introduced by [Yeh \(1998\)](#), who proposed the use of neural networks to predict the compressive strength of high-performance concrete based on 8 input features, such as the densities of cement and water in the mixture, using 1,030 samples (see also [Mišić \(2020\)](#)). The optimization problem associated with **Concrete** can be interpreted as the identification of a concrete composition with maximum compressive strength.

Differently from **Peaks**, optimal solutions for **Wine** and **Concrete** are unknown. Moreover, there is no simple way of evaluating the quality of the solutions produced by our algorithms, as closed-formula expressions to evaluate the objective values of these problems are not available. Nevertheless, our focus is not on the actual quality of our solutions, but on the computational performance of the algorithms when solving the underlying optimization problems.

5.1.2 Families of Instances

We generate two families of instances for our experiments. We refer to the first set as **Medium-sized**, and it consists of three random instances for each combination of $L \in \{1, 2, 3\}$, $n \in \{10, 20, 30\}$, and $e \in \{1, 2, 3\}$ for each of the three benchmark problems described above; therefore, **Medium-sized** contains 243 instances. **Large** is our second family of instances, and it is composed of three random instances for each combination of $L \in \{1, 2, 3\}$, $n \in \{15, 30, 50\}$, and $e \in \{5, 7\}$ for the **Peaks** problem, i.e., **Large** has 54 instances in total. Observe that for $(3, 50, 7)$, the largest configuration, there are $3 \times 50 \times 7 = 1050$ neurons controlled by a ReLU activation function, which in turns correspond to the number of auxiliary binary variables in the formulation.

5.1.3 Training and selection of neural networks

To prepare the dataset for Peaks problem, we sample 1000 data points from the domain of Peaks function and evaluate them using (15). The datasets for Wine and Concrete problems are downloaded from [Dua and Graff \(2017\)](#), consisting of 1600 and 1030 records respectively. We randomly split 70% of the dataset as the training set which will be used to train all neural networks for the same problem. Following the standard practice of neural network training ([Bishop et al. 1995](#)), a min-max normalization is applied to the training data to scale independent and

target variables to the range $[0,1]$ that is also the domain of x in the optimization model. Training an ensemble with $e = 1$ is essentially the same as training a single NN, so we use the Multi-layer Perceptron regressor function `MLPRegressor` in Scikit-learn to train the neural network in these cases (Pedregosa et al. 2011). Since our purpose is to prepare instances for the optimization model instead of improving prediction accuracy of the neural network, we minimize the hyperparameter tuning process by setting 3000 epochs for all neural networks such that the training algorithm will eventually converge, and using Adam training algorithm (Kingma and Ba 2014) with default parameters specified in `MLPRegressor`. For ensembles with more neural networks, we use `MLPRegressor` combined with `BaggingRegressor`, an implementation of bagging ensemble method in Scikit-learn (Pedregosa et al. 2011). After the training is completed, we store the learned weights and bias of the neural networks for the next-step optimization.

5.1.4 Implementation details

We implemented B&C using callbacks, as described in Anderson et al. (2020). In preliminary computational experiments we found that imposing an upper limit on the total number of generated cuts helps to reduce the total computation time. We set this upper limit to 25,000 and compute the values for LB and UB by solving 2 LPs for each neuron.

Algorithm E-NN uses our proposed targeted strong bounds procedure to compute the values of LB and UB, and generates valid inequalities (10) via lazy cuts every time that a feasible integer solution is found. After fine tuning the parameters for E-NN on a subset of instances, we set $K = 1000$, $\tau = 0.01$, and a time limit of 10 seconds for the MILPs in the targeted strong bounding procedure. We remark that the computational times reported in figures and tables include any time spent in preprocessing, computing bounds, and separating cuts or valid inequalities.

5.2 Comparison with the State-of-the-Art Algorithm

The performance of B&C and E-NN on the Medium-sized instances is summarized in Figure 1 and Table 1. Figure 1 shows a cumulative plot for B&C and E-NN in terms of execution time and optimality gap. Namely, on the left side of Figure 1, each point in a curve indicates the number of instances (y-axis) that were solved to optimality by the respective algorithm within the amount of time indicated in the x-axis. On the right side, the curves show the number of instances solved within the optimality gap indicated in the x-axis. Observe that the gap for instances solved to optimality is always equal to zero, so the right side of the plot is a natural extension of its left side.

Figure 1 shows that the cumulative performance of E-NN is superior to that of B&C. Whereas both algorithms solve a significant number of instances within seconds, the plots suggest that the harder instances had a more significant impact on the performance of B&C. These observations can be further investigated with the support of Table 1, which aggregates the results for the Medium-sized instances by problem, number e of ensembles, and number L of intermediate layers; these parameters are presented in the first three columns of the table. The table omits the number n of nodes per layer, and as we have three random instances per configuration, each entry aggregates the results of 9 instances. For each algorithm we report the average execution times (in seconds, with fractional values rounded up, and using “3,600” for instances that reached the time limit), the number of instances solved to optimality, and the average gap of the instances that were not closed within 3,600 seconds (with “-” representing cases where all instances were solved).

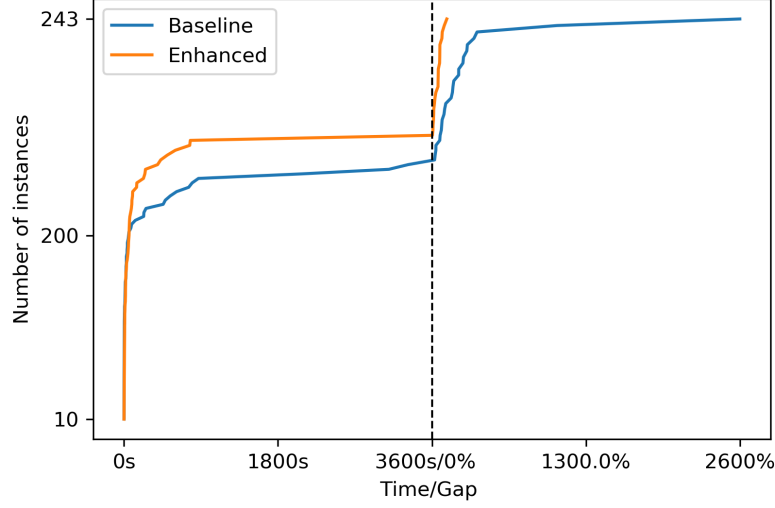


Figure 1: Cumulative performance plot comparing B&C and E-NN on the Medium-sized instances.

Table 1: Summary of results of B&C and E-NN for the Medium-sized instances.

Instance Problem	e	L	Baseline (B&C)			Enhanced (E-NN)		
			Time(s)	Solved	Gap	Time(s)	Solved	Gap
Wine	1	1	1	9	-	1	9	-
		2	3	9	-	14	9	-
		3	18	9	-	52	9	-
	2	1	1	9	-	2	9	-
		2	1152	7	44%	547	8	13%
		3	1325	6	217%	1257	6	48%
	3	1	4	9	-	8	9	-
		2	1698	5	151%	1619	5	43%
		3	2405	3	753%	2405	3	78%
Concrete	1	1	1	9	-	1	9	-
		2	1	9	-	3	9	-
		3	11	9	-	34	9	-
	2	1	1	9	-	1	9	-
		2	162	9	-	44	9	-
		3	1298	6	138%	1218	6	22%
	3	1	1	9	-	1	9	-
		2	913	7	33%	166	9	-
		3	2369	4	224%	1698	5	40%
Peaks	1	1	1	9	-	1	9	-
		2	1	9	-	1	9	-
		3	1	9	-	2	9	-
	2	1	1	9	-	1	9	-
		2	1	9	-	2	9	-
		3	13	9	-	10	9	-
	3	1	1	9	-	1	9	-
		2	5	9	-	3	9	-
		3	659	8	27%	19	9	-

The results presented in Table 1 show that our enhanced algorithm scales better than the

baseline. In addition to solving to optimality at least one instance more per problem type than B&C, E-NN delivers considerably better gaps (in some cases, almost ten times better) for instances with larger values of L and e . Conversely, for scenarios where $e = 1$ or $L = 1$, both algorithms solve virtually all instances within one minute and B&C slightly outperforms E-NN.

Table 1 also allows us to conclude that the relative performances of the algorithms are essentially equivalent in terms of problem type. **Peaks** is clearly easier, with almost all instances being solved within a few seconds by both algorithms; only one instance, associated with the largest values of e and L , could not be solved by B&C. Conversely, the real-world problems are considerably harder; with more features, **Wine** is the hardest problem, but the largest instances of **Concrete** were also challenging. Whereas E-NN does deliver relatively high optimality gaps for some instances, the plots in Figure 1 show that the performance of B&C can be orders of magnitude worse.

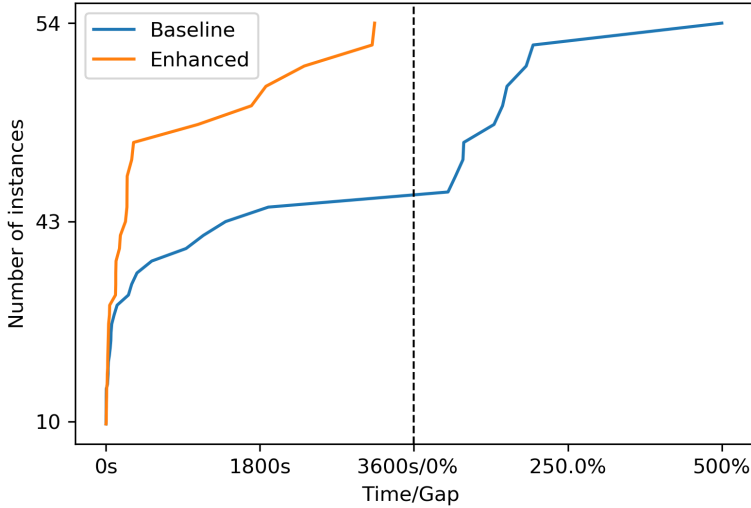


Figure 2: Cumulative performance plot comparing B&C and E-NN on the **Large** instances.

Similar insights are derived from our experiments with the **Large** instances; the cumulative performance plots extracted from these experiments are presented in Figure 2, and the detailed results are presented in Table 2. With larger values of e , these instances are harder for B&C than for E-NN. Namely, whereas E-NN solves all the instances to optimality within 3,600 seconds, B&C delivers poor optimality gaps in scenarios with $L = 3$, and its average solution times are worse than those of E-NN by a factor of at least 2. Therefore, our results suggest that the enhanced approach is consistently superior to the baseline algorithm for optimization over ensembles of neural networks.

Table 2: Summary of results of B&C and E-NN for the **Large** instances.

Instance		Baseline (B&C)			Enhanced (E-NN)		
e	L	Time(s)	Solved	Gap	Time(s)	Solved	Gap
5	1	1	9	-	2	9	-
	2	114	9	-	46	9	-
	3	1889	5	160%	569	9	-
7	1	1	9	-	4	9	-
	2	398	9	-	94	9	-
	3	2426	3	208%	1057	9	-

5.3 Evaluation of the Acceleration Strategies

To assess the effect of each acceleration technique, we compare 4 different versions of our algorithm:

- LPB: Formulation (4) without any valid inequalities and values of LB and UB computed by solving 2 LPs per neuron.
- LPB-VI: Formulation (4) enhanced with valid inequalities (10) and values of LB and UB computed by solving 2 LPs per neuron.
- TSB: Formulation (4) without any valid inequalities and values of LB and UB computed by our targeted strong bounds procedure.
- TSB-VI: Formulation (4) enhanced with valid inequalities (10) and values of LB and UB computed by our targeted strong bounds procedure.

We test the four versions of our algorithm on the 18 instances from the **Large** data set where $n = 50$. Table 3 reports the results for this experiment using the same performance measures as before.

Table 3: Assessing the effect of the acceleration strategies on a subset of the **Large** instances.

Algorithm	Time(s)	Solved	Gap
LPB	1934	10	3547%
LPB-VI	1829	11	587%
TSB	837	18	-
TSB-VI	795	18	-

Table 3 shows that adding valid inequalities (10) when bounds are computed via LPs leads to a moderate reduction in the average computational time and to a considerable decrease in the optimality gap (from 3547% to 587%); as a result, LPB-VI closes one additional instance within the time limit than TSB. In contrast, our proposed targeted strong bounds have a dramatic effect in the number of instances solved and the computational time. Adding valid inequalities (10) in addition to the targeted strong bounds procedure results in a modest reduction of the computational time of about 5% (from 837 seconds to 795 seconds). We conclude that the targeted strong bounds strategy has the most dramatic effect on the computational performance, while the valid inequalities play a modest yet positive role in enhancing the formulation.

We compare the bounds delivered by Tsay et al. (2021)’s progressive bounds tightening procedure with the bounds computed by our targeted bounds strategy (described in §4.1) on the **Large** data set. Table 4 reports the results for this experiment. As in Table 2, we consolidate the results by e and L , which are indicated in the first two columns of Table 4. For each critical neurons $v_j^{i,l}$ identified by our algorithm, we compute its *width* $\omega_j^{i,l}$, which is defined in terms of the bounds of the interval $[LB_j^{i,l}, UB_j^{i,l}]$ containing $h_j^{i,l}$ as

$$\omega_j^{i,l} = UB_j^{i,l} - LB_j^{i,l}. \quad (16)$$

In Table 4 we present the average width “ ω_{LP} ” obtained by solving LPs in the third column and the average width “ ω_{MIP} ” delivered by our bounding procedure. Finally, the fifth and last column is the tightening ratio $\frac{\omega_{LP}}{\omega_{MIP}}$ of our algorithm over the LP approach. We omit ensembles with only one intermediate layer as for those instances $\omega_{LP} = \omega_{MIP}$ (see Tjeng et al. (2019)); observe that this result, combined with the fact that the valid inequalities are not as impactful as the strong bounds, can be used to explain why B&C and E-NN have similar performance when the NNs have a single hidden layer, as presented in §5.2.

As the number of layers increases, the difference in the quality of the bounds becomes more evident. For ensembles with 2 intermediate layers our bounding procedure obtains bound that are on average roughly 20% tighter, while for ensembles with 3 intermediate layers we obtain improvements of almost 50%. As noted in Table 2, these differences in the tightness of the bounds lead to a compelling reduction of the total computational time.

Table 4: Investigating the strength of the bounds obtained via targeted strong bounding

e	L	ω_{LP}	ω_{MIP}	$\frac{\omega_{LP}}{\omega_{MIP}}$
5	2	1.53	1.31	1.18
	3	1.62	1.13	1.48
7	2	1.50	1.30	1.17
	3	1.64	1.14	1.48

6 Conclusion

Optimization models with embedded trained neural networks have been the focus of multiple studies from the literature in the past few years. We propose for the first time to use an ensemble of neural networks instead of a single neural network, as it is well-known that ensembles are superior predictive models.

We study an optimization problem with the objective function represented by an ensemble of neural networks and formulate it as a mixed-integer linear programming problem. We develop valid inequalities derived from a Benders decomposition approach and combine them with a targeted bound tightening procedure to reduce the computational times for the challenging optimization model at hand. Computational results show that our solution methods outperform an state-of-the-art branch-and-cut algorithm both in terms of CPU time and optimality gap, especially for large-sized ensembles of neural networks.

Our work opens different streams for future research. One direction relates to the interplay between the statistical properties of a trained neural network ensemble and its ensuing optimization model. We would like to investigate if predictors with lower MSE values directly result in optimization models with higher solution quality or which statistical performance measures of the predictors play a major role in ensuring that the optimization model produces high-quality solutions. Another line of future research is related with acceleration techniques that exploit information from different networks in the ensemble. Finally, we would like to explore alternative representations of the solution space which could result in tighter formulations (e.g., using decision diagrams to represent the space of feasible binary assignments of the auxiliary z -variables).

References

- Ross Anderson, Joey Huchette, Will Ma, Christian Tjandraatmadja, and Juan Pablo Vielma. Strong mixed-integer programming formulations for trained neural networks. *Mathematical Programming*, pages 1–37, 2020.
- Andrea Bartolini, Michele Lombardi, Michela Milano, and Luca Benini. Neuron constraints to model complex real-world problems. In *International Conference on Principles and Practice of Constraint Programming*, pages 115–129. Springer, 2011.
- J. F. Benders. Partitioning procedures for solving mixed variables programming problems. *Numerische Mathematik*, 4(1):238–252, 1962.
- David Bergman, Teng Huang, Philip Brooks, Andrea Lodi, and Arvind U Raghunathan. Janos: An integrated predictive and prescriptive modeling framework. *arXiv preprint arXiv:1911.09461*, 2019.
- Dimitris Bertsimas, Allison O’Hair, Stephen Relyea, and John Silberholz. An analytics approach to designing combination chemotherapy regimens for cancer. *Management Science*, 62(5): 1511–1531, 2016.
- Max Biggs, Rim Hariss, and Georgia Perakis. Optimizing objective functions determined from random forests. *Available at SSRN 2986630*, 2017.

- Max Biggs, Wei Sun, and Markus Ettl. Model distillation for revenue optimization: Interpretable personalized pricing. In *International Conference on Machine Learning*, pages 946–956. PMLR, 2021.
- Christopher M Bishop et al. *Neural networks for pattern recognition*. Oxford university press, 1995.
- Elena Botoeva, Panagiotis Kouvaros, Jan Kronqvist, Alessio Lomuscio, and Ruth Misener. Efficient Verification of ReLU-Based Neural Networks via Dependency Analysis. *Proceedings of the AAAI Conference on Artificial Intelligence*, 34(04):3291–3299, April 2020. ISSN 2374-3468, 2159-5399. doi: 10.1609/aaai.v34i04.5729. URL <https://aaai.org/ojs/index.php/AAAI/article/view/5729>.
- Leo Breiman. Bagging predictors. *Machine learning*, 24(2):123–140, 1996.
- Rudy Bunel, Ilker Turkaslan, Philip H. S. Torr, Pushmeet Kohli, and M. Pawan Kumar. A Unified View of Piecewise Linear Neural Network Verification. *arXiv:1711.00455 [cs]*, May 2018. URL <http://arxiv.org/abs/1711.00455>. arXiv: 1711.00455.
- Chih-Hong Cheng, Georg Nührenberg, and Harald Ruess. Maximum resilience of artificial neural networks. In *International Symposium on Automated Technology for Verification and Analysis*, pages 251–268. Springer, 2017.
- Paulo Cortez, António Cerdeira, Fernando Almeida, Telmo Matos, and José Reis. Modeling wine preferences by data mining from physicochemical properties. *Decision Support Systems*, 47(4):547–553, 2009.
- Thomas G. Dietterich. Ensemble methods in machine learning. *Lecture Notes in Computer Science (including subseries Lecture Notes in Artificial Intelligence and Lecture Notes in Bioinformatics)*, 1857 LNCS:1–15, 2000. ISSN 16113349. doi: 10.1007/3-540-45014-9\1.
- Dheeru Dua and Casey Graff. UCI machine learning repository, 2017. URL <http://archive.ics.uci.edu/ml>.
- Souradeep Dutta, Susmit Jha, Sriram Sankaranarayanan, and Ashish Tiwari. Output range analysis for deep feedforward neural networks. In *NASA Formal Methods Symposium*, pages 121–138. Springer, 2018.
- Matteo Fischetti and Jason Jo. Deep neural networks and mixed integer linear optimization. *Constraints*, 23(3):296–309, 2018.
- Ian Goodfellow, Yoshua Bengio, and Aaron Courville. *Deep learning*. MIT press, 2016.
- Bjarne Grimstad and Henrik Andersson. ReLU networks as surrogate models in mixed-integer linear programs. *Computers & Chemical Engineering*, 131:106580, December 2019. ISSN 00981354. doi: 10.1016/j.compchemeng.2019.106580. URL <https://linkinghub.elsevier.com/retrieve/pii/S0098135419307203>.
- Inc. Gurobi Optimization. Gurobi optimizer reference manual, 2018. URL <http://www.gurobi.com>.
- Lars Kai Hansen and Peter Salamon. Neural network ensembles. *IEEE transactions on pattern analysis and machine intelligence*, 12(10):993–1001, 1990.
- Guy Katz, Clark Barrett, David L Dill, Kyle Julian, and Mykel J Kochenderfer. Reluplex: An efficient smt solver for verifying deep neural networks. In *International Conference on Computer Aided Verification*, pages 97–117. Springer, 2017.
- Diederik P Kingma and Jimmy Ba. Adam: A method for stochastic optimization. *arXiv preprint arXiv:1412.6980*, 2014.
- Hui Li, Xuesong Wang, and Shifei Ding. Research and development of neural network ensembles: a survey. *Artificial Intelligence Review*, 49(4):455–479, 2018.
- Sheng Liu, Long He, and Zuo-Jun Max Shen. On-Time Last-Mile Delivery: Order Assignment with Travel-Time Predictors. *Management Science*, November 2020. ISSN 0025-1909. doi: 10.1287/mnsc.2020.3741. URL <https://pubsonline.informs.org/doi/abs/10.1287/mnsc.2020.3741>. Publisher: INFORMS.

- Alessio Lomuscio and Lalit Maganti. An approach to reachability analysis for feed-forward ReLU neural networks. *arXiv:1706.07351 [cs]*, June 2017. URL <http://arxiv.org/abs/1706.07351>. arXiv: 1706.07351.
- Velibor V Mišić. Optimization of tree ensembles. *Operations Research*, 68(5):1605–1624, 2020.
- Fabian Pedregosa, Gaël Varoquaux, Alexandre Gramfort, Vincent Michel, Bertrand Thirion, Olivier Grisel, Mathieu Blondel, Peter Prettenhofer, Ron Weiss, Vincent Dubourg, et al. Scikit-learn: Machine learning in python. *the Journal of machine Learning research*, 12: 2825–2830, 2011.
- Artur M Schweidtmann and Alexander Mitsos. Deterministic global optimization with artificial neural networks embedded. *Journal of Optimization Theory and Applications*, 180(3): 925–948, 2019.
- Thiago Serra, Christian Tjandraatmadja, and Srikumar Ramalingam. Bounding and counting linear regions of deep neural networks. In *International Conference on Machine Learning*, pages 4558–4566. PMLR, 2018.
- Thiago Serra, Abhinav Kumar, and Srikumar Ramalingam. Lossless compression of deep neural networks. In *International Conference on Integration of Constraint Programming, Artificial Intelligence, and Operations Research*, pages 417–430. Springer, 2020.
- Vincent Tjeng, Kai Xiao, and Russ Tedrake. Evaluating Robustness of Neural Networks with Mixed Integer Programming. *arXiv:1711.07356 [cs]*, February 2019. URL <http://arxiv.org/abs/1711.07356>. arXiv: 1711.07356.
- Calvin Tsay, Jan Kronqvist, Alexander Thebelt, and Ruth Misener. Partition-based formulations for mixed-integer optimization of trained relu neural networks. *arXiv preprint arXiv:2102.04373*, 2021.
- Sicco Verwer, Yingqian Zhang, and Qing Chuan Ye. Auction optimization using regression trees and linear models as integer programs. *Artificial Intelligence*, 244:368–395, 2017.
- Juan Pablo Vielma. Mixed Integer Linear Programming Formulation Techniques. *SIAM Review*, 57(1):3–57, January 2015. ISSN 0036-1445, 1095-7200. doi: 10.1137/130915303. URL <http://epubs.siam.org/doi/10.1137/130915303>.
- Keliang Wang, Leonardo Lozano, David Bergman, and Carlos Cardonha. A two-stage exact algorithm for optimization of neural network ensemble. In *International Conference on Integration of Constraint Programming, Artificial Intelligence, and Operations Research*, pages 106–114. Springer, 2021.
- Kai Y. Xiao, Vincent Tjeng, Nur Muhammad Shafiullah, and Aleksander Madry. Training for Faster Adversarial Robustness Verification via Inducing ReLU Stability. *arXiv:1809.03008 [cs, stat]*, April 2019. URL <http://arxiv.org/abs/1809.03008>. arXiv: 1809.03008.
- I-C Yeh. Modeling of strength of high-performance concrete using artificial neural networks. *Cement and Concrete research*, 28(12):1797–1808, 1998.
- Zhi-Hua Zhou, Jianxin Wu, and Wei Tang. Ensembling neural networks: many could be better than all. *Artificial intelligence*, 137(1-2):239–263, 2002.